Comparative study of various modulation schemes used in indoor VLC

by
Surbhi Maheswari

Under the Supervision of Dr. Anand Srivastava

Indraprastha Institute of Information Technology New Delhi
June, 2017

Comparative study of various modulation schemes used in indoor VLC

by
Surbhi Maheswari

Submitted
in partial fulfillment of the requirements for the degree of
Master of Technology

to

Indraprastha Institute of Information Technology, New Delhi
June, 2017

Certificate

This is to certify that the thesis titled **Comparative study of various modulation schemes used in indoor VLC** being submitted by Surbhi Maheshwari to the Indraprastha Institute of Information Technology Delhi, for the award of the Master of Technology, is an original research work carried out by her under my supervision. In my opinion, the thesis has reached the standards fulfilling the requirements of the regulations relating to the degree.

The results contained in this thesis have not been submitted in part or full to any other university or institute for the award of any degree/diploma.

June, 2017

Anand Srivastava
Department of Electronics and Communications
Indraprastha Institute of Information Technology Delhi
New Delhi 110020

Acknowledgments

I would like to thank Dr. Anand Srivastava for giving me this opportunity to work on this project, and for providing with all support and guidance. I would also like to express my gratitude to parents and friends for their constant support.

Abstract

This thesis work proposes analysis and simulation of 5G multi-carrier transmission schemes based on generalized frequency division multiplexing (GFDM) along with existing optical orthogonal frequency division multiplexing (O-OFDM) for indoor visible light communication (VLC).The aim is to overcome the inherent drawbacks of the commonly used optical orthogonal frequency division multiplexing (O-OFDM) schemes. Various performance metrics are analyzed and compared with O-OFDM schemes. It is found that proposed scheme has better spectral and power efficiency. Also its symbol error rate (SER) performance is found to be superior over optical OFDM counterparts under line-of-sight(LOS) optical channel. Simulation results based on SER, peak-to-average-power-ratio (PAPR),and numerical analysis on spectral efficiency validate the performance of the proposed schemes. As GFDM is being actively considered for LTE-A like 5G systems, it is expected that the O-GFDM based VLC system will very well gel with next generation wireless systems to offer seamless end-to-end communication services and will provide greater flexibility using software defined networking.

Thesis work also includes a DFT-precoded optical OFDM modulation scheme to overcome the inherent drawback of high PAPR of DCO-OFDM and this scheme is compared with DCO-OFDM in context of SER and PAPR performances.Its better SER performance and reduced PAPR make it suitable as the substitute of DCO-OFDM.

Keywords:Direct current offset optical orthogonal frequency division multiplexing (DCO-OFDM), Asymmetrically clipped optical orthogonal frequency division multiplexing (ACO-OFDM), Generalized frequency division multiplexing (GFDM), Symbol error rate (SER), Spectral efficiency, Peak-to-averagepower- ratio (PAPR).

Contents

1 Introduction **3**

2 Visible Light Communication system **6**

2.1 LED 6

2.2 VLC basic structure 9

2.3 Channel Modelling 11

2.4 Receivers 12

3 Modulation Schemes **13**

3.1 DCO OFDM 13

3.2 ACO-OFDM 15

3.3 OGFDM 16

3.3.1 OGFDM-DC 17

3.3.2 OGFDM-NDC 21

4 DFT Precoded Optical OFDM **24**

4.1 DFT precoded optical OFDM 24

5 Mathematical analysis of Spectral efficiency **26**

6 Simulation and Results **28**

6.0.1 SER 28

6.0.2 PAPR 29

6.0.3 Complexity 30

6.1 Simulation results of proposed modulation scheme 35

6.1.1 SER 35

6.1.2 PAPR 35

Conclusion **38**

Bibliography **39**

Chapter 1

Introduction

Visible light optical communication is a form of telecommunication, which uses light to carry information. This form of optical wireless communication (OWC) has immense potential of high speed data communication, thanks to the availability of nearly 670 THz of license-free spectrum. In visible light communication (VLC), signals occupy visible light spectrum from 375 nm to 750 nm. The net resultant bandwidth is nearly 10,000 times higher than the Radio Frequency bandwidth.

VLC uses Light emitting diodes (LED) as transmitters, and photo-diodes as receivers. The LED which operates in visible light spectrum serves dual purpose of illumination and communication, making VLC preferred choice in indoor wireless communication scenarios. This is how a VLC system works: LED transmits the intensity modulated over the air, and a detector detects the change in the brightness level of that modulated signal, to decodes back the signal. We essentially start with an electrical signal, convert to optical signal and send it using an LED, receive the optical signal at receiver, convert it back from optical to electrical. There are further many variations in how we modulate the signal in optical domain, On-Off keying being the most basic technique. In On-off keying, we represent a binary one as LED bulb switched on, binary zero as LED bulb off. Thus a stream of ones and zeros in electrical domain, will be represented as LED bulb switching on and off for corresponding bits. Moreover, since the detector works on the difference of brightness level, the constant ambient light is cancelled out. Fig.1.1 shows the wavelength bands of different waves such as Gamma rays, X-rays, UV and Visible light.

Communication using visible light is not a new concept. Most ancient form of visible light communication can be traced by to an era, when people used fires beacons and smoke signal to convey messages to farther distances. The very first documented use of visible light in communication can be credited to Alexander Graham Bell, for his photophone in 1880 [2]. He conducted an experiment to demonstrate voice data transmission over sunlight to a distance of 200 meters. Use of fluorescent light was also used for low data rate transmission [3]. In 2001, Twibright Labs developed RONJA (Reasonable Optical near Joint Access) a free space optical communication

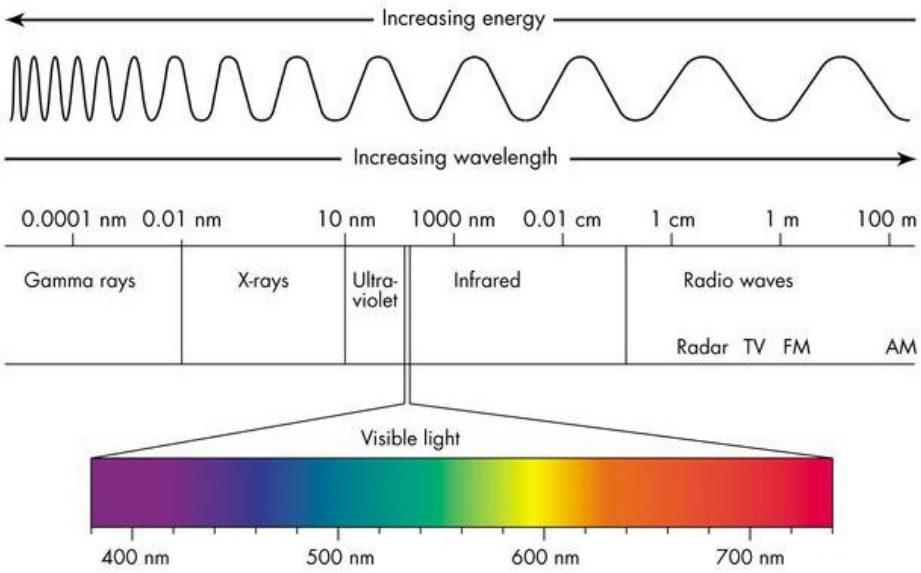

Figure 1.1: EM spectrum [1]

network over 1.4 kms of distance [4]. The use od white LED's for communication was shown by Tanaka et al. in 2000 [5]. in 2003, a Visible light communications consortium (VLCC) was established, with main aim to standardize VLC technologies [1]. Project OMEGA in 2010 aimed at developing home access optical wireless network to work along with RF technology [1] . There are multiple research groups working in visible light communication, and some have thier own research companies setup, such as pureLiFi from University of Edinburg, Oxford University , Boston University [1].

Why VLC?

VLC finds it's usage in multiple useful applications, such as car to car communication, traffic light systems, indoor positioning system, data communications in warehouses, factories and aircraft, in home Wi-Fi connectivity. VLC has multiple advantages over RF, which can be summarized in below mentioned points

1. **Interference**: VLC is inherently safer as compared to RF, since use of RF creates restriction in some industries, in aircraft [6]. VLC does not interfere with existing RF signals.

2. **Safety**: RF signals are considered to be harmful (still debatable), but VLC poses no such know risk to humans. Infrared also poses risk to eye and skin, when used at high powers.

3. **Energy Efficiency**: LED bulbs are more efficient then ever, and using such transmitters saves energy by reusing the same light for illumination and data transmission.

4. **Reuse**: Since LEDs used in VLC gives a confined and directional output, the spatial re-usability increases for VLC, and more VLC links can be used in close proximity.

5. **RF spectrum**: There is finite RF spectrum available, which is expensive and is becomes scares due to the exponentially growing consumer demand of higher bandwidth. VLC is proposed as a suitable alternative to RF, thanks to availability of unlicensed spectrum, which is 10,000 times more as compared to RF. To get a comparison of spectrum of two technologies, radio waves lye in range of 3 kHz to 300 GHz, while visible light lye in range of 400 THz to 780 Thz [1].

6. **Security**: VLC is considered more secure than RF, since visible light is confined inside walls, while RF signals are able to cross walls and are vulnerable to snooping.

Comparison of VLC with RF and IR communication

Table 1.1: Comparison of RF, Infrared and visible light communication systems [1]

Parameter	**RF**	**IR**	**VLC**
Safety	Intensity Regulated	Intensity Regulated	Unregulated
Noise	Low	High	High
Security	Limited	High	High
Coverage	Wide	Limited	Limited
Multipath	High	Low	Low
System Complexity	High	Low	Low
Electromagnetic Interference	Yes	No	No
Infrastructure	Access points	Access points	Illumination
Power Consumption (Short range link)	Medium	Low	Lowest

Table 1.1 shows the comparison of VLC, RF and Infrared communication. It summaries the pros and cons of VLC as compared to RF and IR. Considering the positive points, VLC is not intensity regular, has high security, lo multipath, low system complexity, zero electromagnetic interference and lowest power consumption. If we come to the negatives of VLC, it has higher noise and limited coverage. To summaries, VLC offers much better alternative to RF and infrared, and decision to opt for VLC depends on the scenario in which it would be implemented, where pros would overcomes it's cons.

Chapter 2

Visible Light Communication system

2.1 LED

The usage of incandescent lamps is lowering down with the passage of time due to their poor energy efficiency.Compact fluorescent (CFL) bulbs were introduced to improve energy efficiency. They have longer life as compared to incandescent bulbs.They are not suitable in high speed switching because of their instant switching. The concept of LEDs is the new one. LEDs have longer lifetime, more energy efficiency.LEDs are not harmful as they do not contain hazardous substance like mercury. LEDs have one disadvantage which is its high cost.

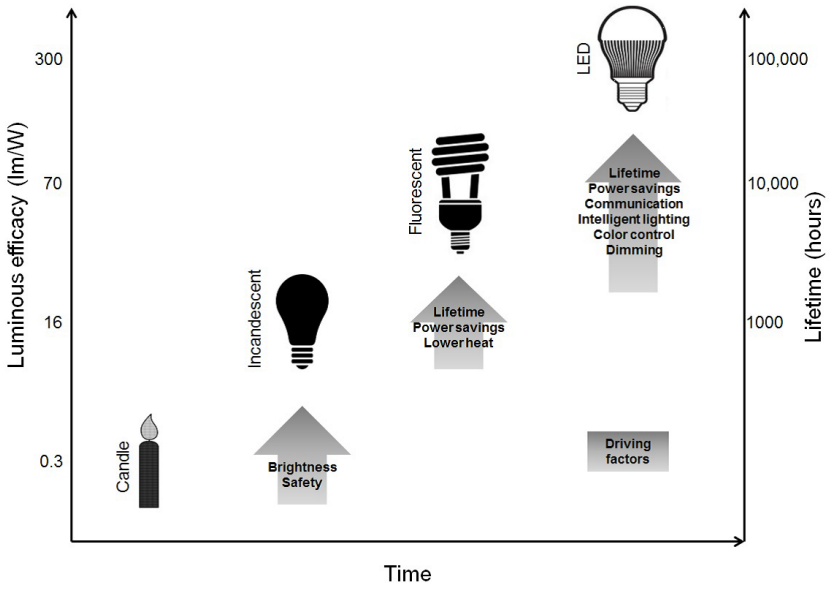

Figure 2.1: Progress in illumination [1]

The progress in illumination technologies is shown in Fig.2.1. The horizontal axis represents the time with order in which products came into existence whereas products lifetime is represented by right vertical axis and luminous efficacy by left vertical axis i.e. the lumens produced

per watt of energy supplied. LED overcomes the other existing technology because of its highest life time, highest luminous efficacy, and benefits of power saving. It is used in communication, intelligent lighting, colour control and dimming.

LED is a solid state semiconductor device which coverts the electrical energy into the optical energy. Nowadays LEDs are categorized based on their advantages and disadvantages. The comparison of types of LED is shown in table 2.1 . Karunatilaka et al. in [1] has given a detailed comparison of types of LEDs.

Table 2.1: Comparison of different types of LEDs [1]

Parameter	pc-LED	RGB LED	μ-LED	OLED
Bandwidth	3-5 MHz	10-20 MHz	300 MHz	1 MHz
Efficacy	130 lm/W	65 lm/W	NA	45 lm/W
Cost	Low	High	High	Lowest
Complexity	Low	Moderate	Highest	High
Application	Illumination	Illumination	Bio-sensors	Display

PC-LEDs: These are called as white light LED because of they emit white light. PC-LED consists of a single blue Indium Gallium Nitride (InGaN) LED chip, and Yttrium Aluminium Garnet (YAG) phosphor coating. The phosphor coating converts the blue light to red and green, while the some part of the blue light is leaked out and the mixture of red, green and blue light produces white light (Fig.2.2 and 2.3). They have low cost and less complexity, but lower bandwidth because of the poor phosphor conversion efficiency.

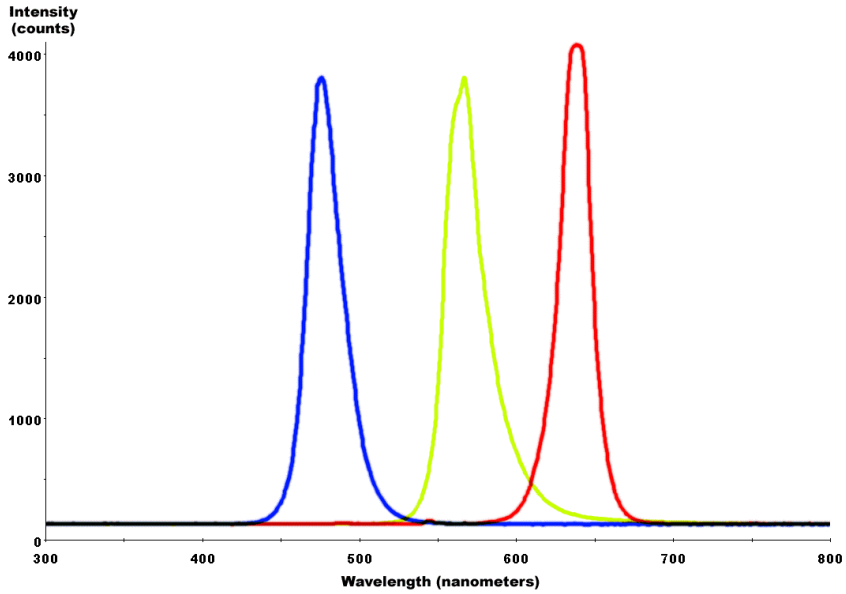

Figure 2.2: [7]

RGB LEDs:Three or more LED chips are used by RGB LEDs.These LEDs emit independent colours, typically Red, Green and Blue (RGB), and produce white light. They have higher

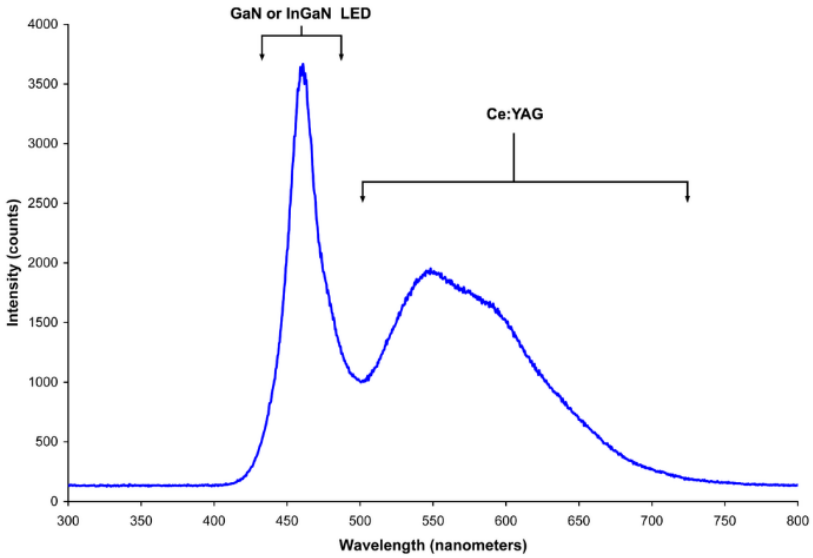

Figure 2.3: [8]

bandwidth if compared with pc-LEDs and have the demerits of lower efficacy along with higher cost.

Micro LEDs (μ-LED): Micro LEDs consist of AlGaN. Basically they are micro-light emitting diode arrays, and are used in display panels, which allows high density parallel communication. They possess low capacitance which results higher bandwidth. Moreover, these LEDs have small size. These LEDs are more complex and costly.

OLED: Light is produced by Organic Light Emitting Diodes (OLEDs) using organic layer between positive and negative carriers. They are generally used in flat panel displays. They cannot be used for illumination purposes, due to low luminous efficacy of 45 lm/W. This efficacy was obtained at cost of reduced lifetime (from 50,000 hours to 8000 hours) [9].

Thus pc-LEDs and RGB LEDs are most appropriate options for illumination and transmission.

2.2 VLC basic structure

Generally, line of sight (LOS) configuration is employed by a VLC link because of its illumination purpose. Incoherent light is emitted by LEDs hence it leads to intensity modulation (IM) in which transmitted signal is modulated into instantaneous optical power of LED. Input forward current controls the radiant intensity through LED.

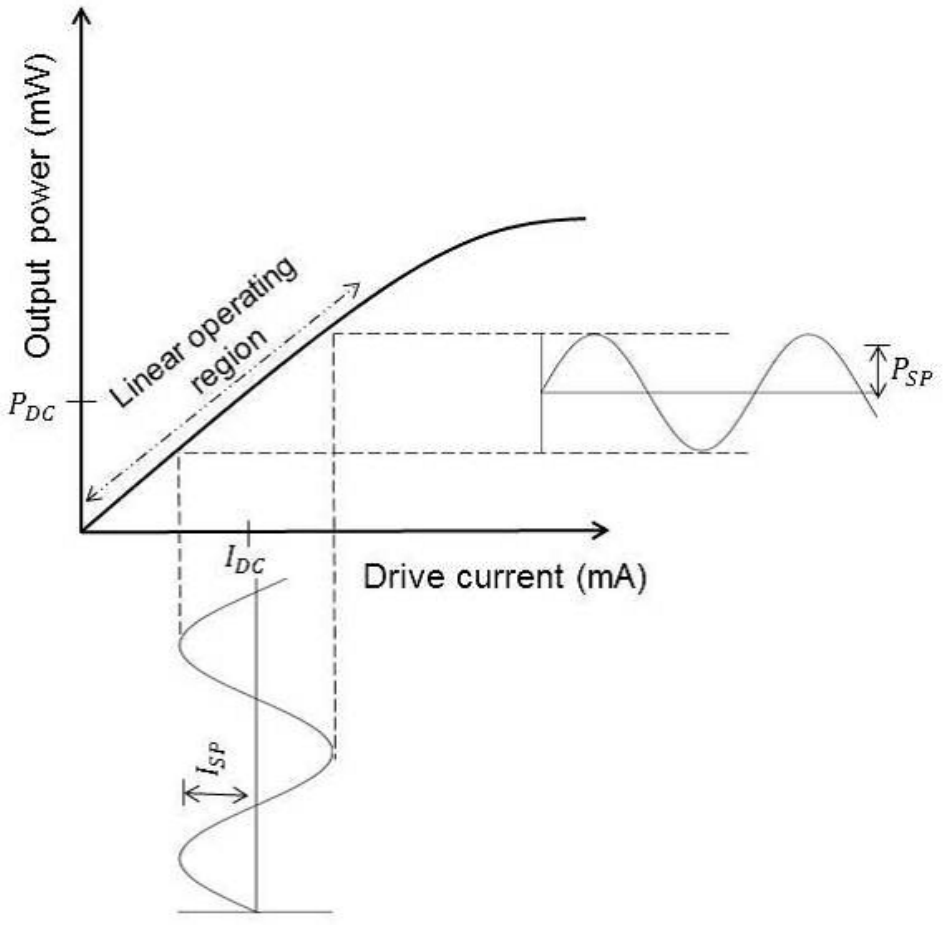

Figure 2.4: Driver current v/s Output Power in LED [1]

Relationship between the input current and the output power is depicted in Fig.2.4. The net input current to LED I_L can be expressed as a summation of I_{DC} and I_{SP}, where I_{DC} and I_{SP} are the DC bias current and the current swing respectively. This net input current I_L generates a net output optical power P_{output}. P_{output} is the summation of P_{DC} and P_{SP} where P_{DC} and P_{SP} are the DC power and power swing respectively. The relationship between input current and output power is linear for a certain range. LED should be operated in its dynamic range or the linear range so that clipping of signal should not occur.

Since intensity modulation (IM) is used at the transmitter side so direct detection (DD) is the suitable method at the receiver side. A photodiode is used in the direct detection method, which converts the incident optical power into proportional current. Moreover,Higher modulation frequency should be used, so that flickering is not sensed by the human eye in LED. A certain lighting standards should be followed for illumination purpose. According to these standards, 400-1000 lux of illumination levels are required in the working area. These standards vary in countries [10].

A general VLC link structure is shown in Fig.2.5, where input signal to LED is in electrical domain, and LED converts the electrical signal into optical domain.The optical signal travels through a channel, and it is received by the photo detector, which converts the received optical signal into electrical. At the photodetector, shot noise and thermal noise are added.

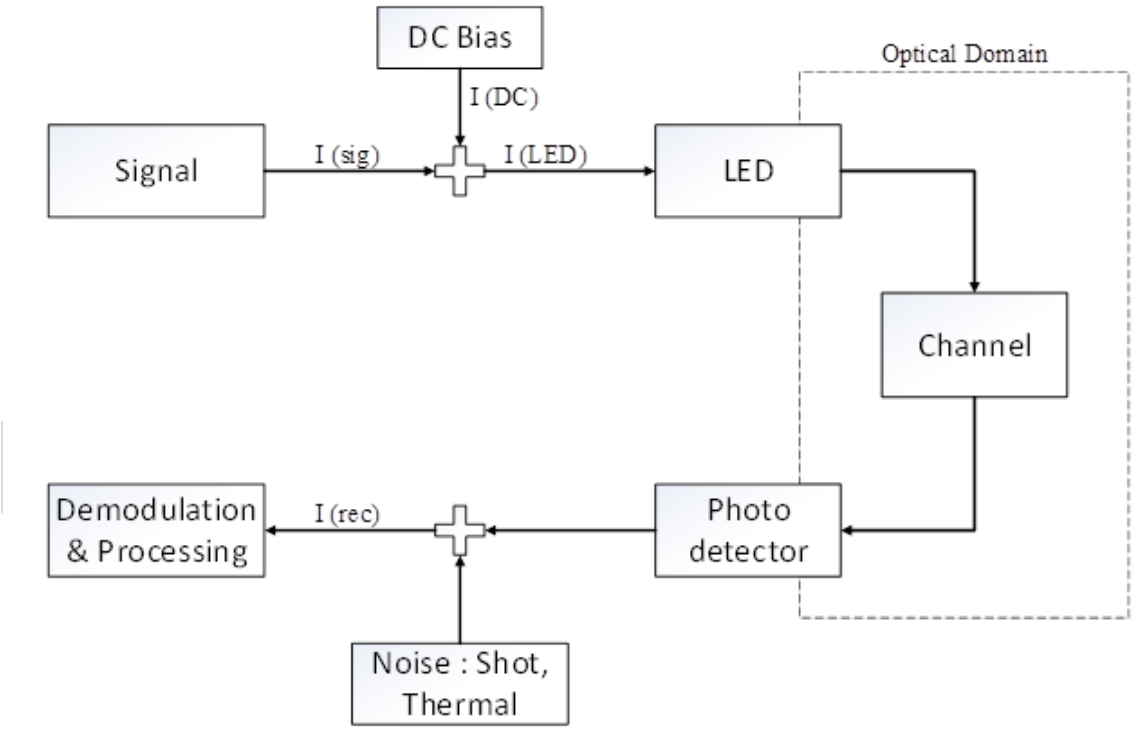

Figure 2.5: VLC link structure

2.3 Channel Modelling

In the following section, assuming a Line of sight scenario, channel modeling is discussed in detail. The channel impulse response approximately can be expressed as

$$h(t;S,R) \approx \frac{mode+1}{2\Pi}\cos^{mode}(\phi)d\omega * rect(\frac{\theta}{FOV})\delta(t-\frac{R}{c}) \tag{2.1}$$

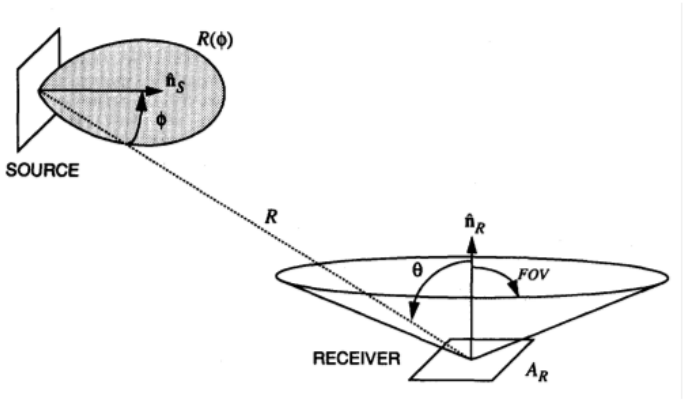

Figure 2.6: Geometry of source and detector without reflectors [11]

where S is source,R is receiver, FOV is the field of view, mode is the mode number associated with the directivity of the source, c is the speed of light and R is the separation distance between transmitter and receiver. Source S is defined as $S = \mathbf{r}_S, \mathbf{n}_s, mode$ where $\mathbf{r}_S$ is the position and $\mathbf{n}_s$ is the orientation of the source. The photo-detector is defined as $R = \mathbf{r}_R, \mathbf{n}_R, A_R, FOV$ where $\mathbf{r}_R$ is the position, $\mathbf{r}_R$ is the orientation and A_R is the receiver area. The solid angle subtended by the receivers differential area is given as

$$d\omega \approx \frac{\cos(\theta)A_R}{R^2} \tag{2.2}$$

θ is the angle between $\mathbf{n}_R$ and $(\mathbf{r}_S - \mathbf{r}_R)$

$$\cos(\theta) = \mathbf{n}_R.\frac{(\mathbf{r}_s - \mathbf{r}_R)}{R} \tag{2.3}$$

ϕ is the angle between $\mathbf{n}_s$ and $(\mathbf{r}_R - \mathbf{r}_s)$

$$\cos(\phi) = \mathbf{n}_s.\frac{(r_R - r_S)}{R} \tag{2.4}$$

The function $rect(l)$ is defined as

$$rect(l) = \begin{cases} 1 for\, |l| \leq 1 \\ 0 for\, |l| > 1 \end{cases} \tag{2.5}$$

The channel equation can be written as

$$y = r.(x * h) + \widetilde{n} \tag{2.6}$$

where y is received signal, r is the receiver responsivity factor, x is the input power signal, h is channel transfer function and $\widetilde{n}$ is the noise [11].

2.4 Receivers

A typical receiver in a VLC system convert the incident optical power to electrical current, in accordance to detector's responsivity. There are two types of photodetector used in VLC, PIN and Avalanche photodetector (APD). APD has advantage over PIN detector, in term of higher gain, which makes it the preferred choice for scenarios with weak optical power incident on detector. On the other hand, PIN are also preferred over APD, due to their lower cost, higher temperature tolerance and lower shot noise. Silicon PD are well suitable for VLC based applications, due to their higher sensitivity in visible light spectrum.

Chapter 3

Modulation Schemes

3.1 DCO OFDM

OFDM is a modulation technique which can be used to get the high data rates by utilizing the multiple subcarriers to transmit the data streams. Since VLC uses intensity modulation in which signal should be real and unipolar. To achieve this, Hermitian symmetry and a DC bias is used in OFDM. A DC offset is used in this technique so this is called as DC Offset OFDM (DCO-OFDM). Block diagram of DCO-OFDM is shown in the Fig.3.1. Input data stream is modulated by quadrature amplitude modulation (QAM). If 2N number of total subcarriers are used to transmit the data then only N number of subcarrier are used to carry the modulated data signals. Rest half of the subcarriers i.e. N are used to carry the complex conjugate of these modulated signals. After the IFFT operation, real valued signals are obtained which are serially transmitted. A DC-offset (implemented in practice as a dc-bias current to drive the LED transmitter) is added to the generated time-domain waveform to convert the signal into a unipolar form and is then transmitted [12]. An OFDM symbol in RF communication is a vector, which consists of a set of N subcarriers. Discrete OFDM symbol vector x is obtained in the time-domain after IFFT operation , which is given by

$$x_m = \frac{1}{N}\sum_{k=0}^{N-1} X_k e^{\frac{j2\pi km}{N}}, for 0 \leq m \leq N-1 \tag{3.1}$$

where N is the size of IFFT and X_k is the symbol of the kth subcarrier. The corresponding FFT conversion of the equation (3.1) can be expressed as

$$X_k = \frac{1}{N}\sum_{k=0}^{N-1} x_m e^{-\frac{j2\pi hm}{N}}, for 0 \leq k \leq N-1 \tag{3.2}$$

A complex valued signal is expressed in equation (3.1). This OFDM symbol cannot be used in LED based VLC systems in which intensity modulation and direct detection (IM/DD) is

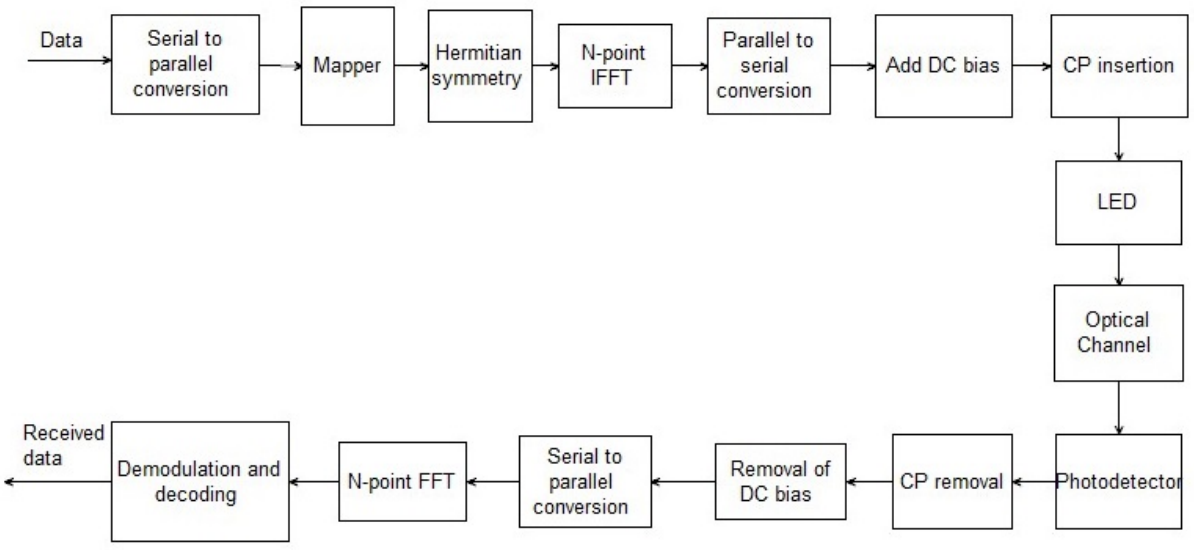

Figure 3.1: Block diagram of DCO-OFDM.

utilized. To get the real valued signal after IFFT operation, hermitian symmetry is used. Hermitian symmetry is nothing but the complex conjugate copy of the first N-subcarriers. These hermitian symmetric values are added to the other half of the IFFT frame. So the total elements of the new IFFT input vector, X_H are given as

$$X_H = \begin{bmatrix} X_0 & X_1 & X_2 & ... & X_{N-1} & X_N & X^*_{N-1} & ... & X^*_2 & X^*_1 \end{bmatrix} \tag{3.3}$$

Where putting the DC values, X0 = XN = 0. DCO OFDM symbol is obtained after the 2N-point IFFT operation. Equation (1) can be rewritten as

$$x_m = \frac{1}{N} \sum_{h=0}^{2N-1} X_{H,h} e^{\frac{j2\pi hm}{N}}, for 0 \leq m \leq 2N-1 \tag{3.4}$$

where h is the h^{th} subcarrier symbol of X_H. The OFDM symbol is a periodic function with a period, $T_p = \frac{1}{\Delta f}$, and Δf is the subcarrier spacing which is given by

$$\Delta f = \frac{B}{N-1} \tag{3.5}$$

where B is the signal modulation bandwidth. At the receiver, a fast Fourier transform (FFT) operation performs the conversion from the time to the frequency domain and each element of the FFT output Y_h is given by

$$Y_h = \sum_{m=0}^{N-1} y_m e^{-\frac{j2\pi hm}{N}}, for 0 \leq h \leq 2N-1 \tag{3.6}$$

where y is vector consists of a set of amplitudes of the received time-domain signal of length 2N. In an additive white Gaussian noise (AWGN) channel, the transmitted and the received signal are given by

$$y = x + n_{AWGN} \tag{3.7}$$

where n_{AWGN} is AWGN noise component, by substituting (3.6) in (3.5),

$$Y_h = \sum_{m=0}^{2N-1} x_m e^{-\frac{j2\pi hm}{N}} + \sum_{m=0}^{2N-1} n_{AWGN,m} e^{-\frac{j2\pi hm}{N}}, for 0 \leq h \leq 2N-1 \tag{3.8}$$

where x_m and $n_{AWGN,m}$ are the signal and noise amplitude of the m-th point of the 2N point time domain signal. $N_{AWGN,h}$ is a Gaussian noise component of the h-th FFT output at the receiver is given by

$$N_{AWGN,h} = \sum_{m=0}^{2N-1} n_{AWGN,m} e^{-\frac{j2\pi hm}{N}}, for 0 \leq h \leq 2N-1 \tag{3.9}$$

therefore, Equation (3.7) can be reduced to

$$y_h = x_h + N_{AWGN,h} \tag{3.10}$$

The intensity modulated signals travel through the optical channel and are received by the photodetector. Photodetector converts the optical signal into the electrical form. The signals are serial to parallel converted and are passed through the FFT block. QAM demodulation is used to obtain the information bits. This method is spectrally efficient in indoor VLC. Since IFFT operation is done so a large DC bias is needed in this technique. It causes high peak-to-average-power-ratio (PAPR) so this method is less power efficient. A high PAPR causes distortion in the received signal [12]. The bit rate of DCO-OFDM is given by

$$R_{DCO} = \frac{N/2}{(T + T_{CP})} log_2 M \tag{3.11}$$

where T and T_{CP} are one time slot and CP duration respectively.

3.2 ACO-OFDM

In scenarios of importance to power efficiency, ACO-OFDM is preferred over DCO-OFDM, primarily due to low PAPR of ACO-OFDM as compared to DCO-OFDM. ACO-OFDM is considered to be more power efficient than the conventional DCO-OFDM, since we require an additional DC bias in case of DCO-OFDM, which is usually not the required for ACO-OFDM. The block diagram of ACO-OFDM is shown in Fig.3.2. There are some small yet significant

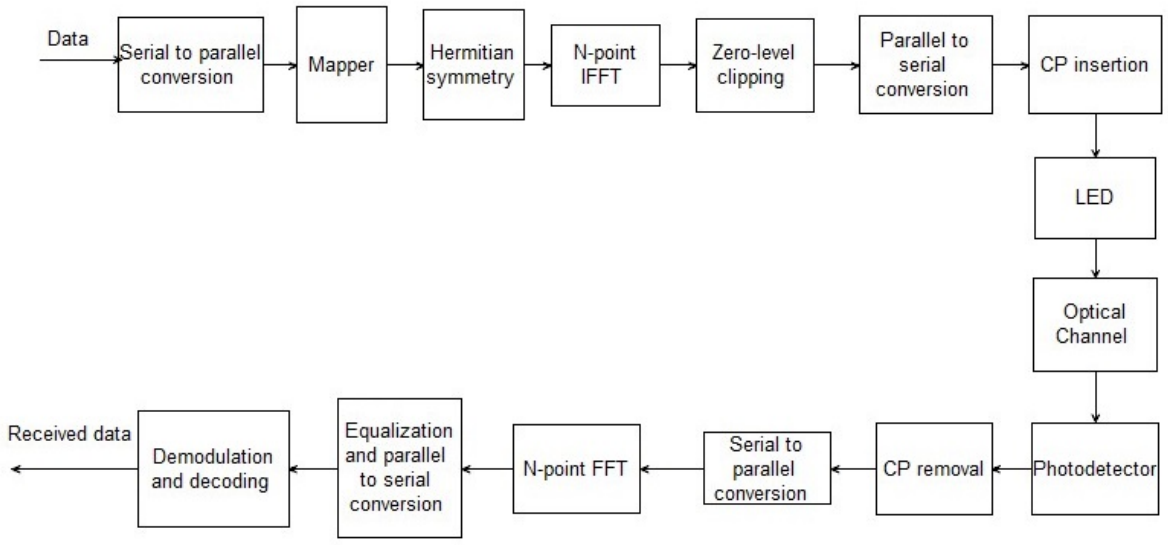

Figure 3.2: Block diagram of ACO-OFDM.

differences between ACO-OFDM and DCO-OFDM. Firstly, for DCO-OFDM, all subcarriers carries information, whereas in ACO-OFDM, the information data is transmitted only through the odd numbered subcarriers and even numbered subcarriers does not contain any information. For transforming the signal to unipolar, we provide a DC bias for DCO-OFDM, and clip the negative signal for ACO-OFDM. For ACO-OFDM it is already proved by other researchers [ref]., that clipping of negative signal does not result in signal loss, and clipped part can be recovered at receiver The unipolar signals are transmitted through the optical channel and received by the photodetector. Photodetector converts the optical energy into the electrical domain and the information data is recovered through FFT operation, demodulation and decoding. ACO-OFDM has a drawback that it has less spectral efficiency if compared with DCO-OFDM, since DCO-OFDM is more spectral efficient [**?**, 13–17].The bit rate of ACO-OFDM is given by

$$R_{ACO} = \frac{N/4}{(T + T_{CP})} log_2 M \tag{3.12}$$

where T and T_{CP} are one time slot and CP duration respectively.

3.3 OGFDM

Generalized frequency division multiplexing (GFDM) is a new candidate technique for the fifth generation (5G) standard based on multibranch multicarrier filter bank in RF wireless communication. It is the generalization of traditional OFDM with several added advantages like the low PAPR (peak-to-average-power-ratio) and higher spectral efficiency. There is no existence of any system model based on GFDM in optical wireless communication based on the study. In this thesis, we propose a flexible multi-carrier optical generalized frequency division

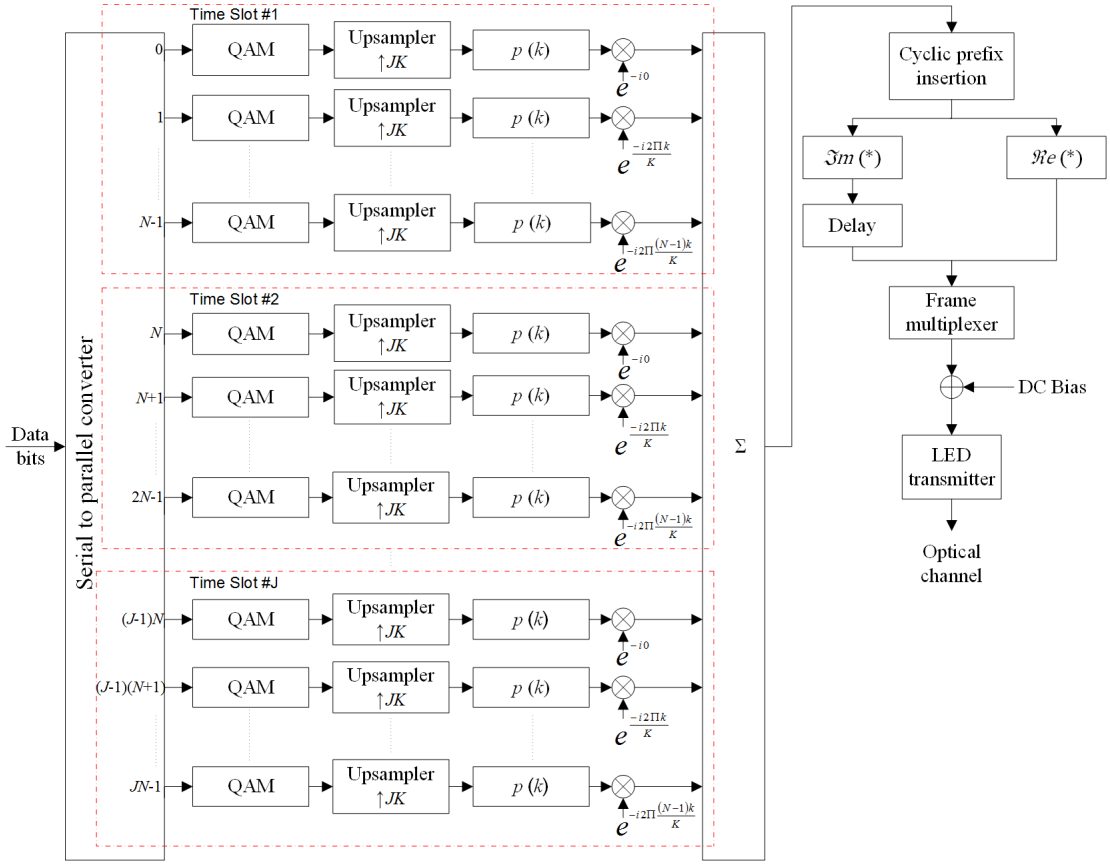

Figure 3.3: Block diagram of OGFDM-DC transmitter.

multiplexing (OGFDM) transmission scheme with and without DC bias. The proposed scheme is evaluated on the basis of symbol error rate (SER),peak-to-average-power-ratio (PAPR) and spectral efficiency which makes it suitable for next generation optical wireless communication.

3.3.1 OGFDM-DC

Transmitter

The block diagram of DC biased OGFDM transmitter is shown in Fig.3.3. The input data bits are converted into NJ data streams where N is total number of subcarriers and J is total number of time slots. The input data bits are divided into NJ data streams and are sent to NJ independent M-QAM mappers. Each modulated data symbol is represented as $s_{n,j}$ where $n = 0, 1, 2, , N-1$ and $j = 0, 1, 2, , J-1$.

O-GFDM frame structure is represented in matrix form as given below

$$\mathbf{S} = \begin{bmatrix} s_{0,0} & s_{0,1} & \cdots & s_{0,J-1} \\ s_{1,0} & s_{1,1} & \cdots & x_{1,J-1} \\ \vdots & \vdots & \ddots & \vdots \\ s_{N-1,0} & s_{N-1,1} & \cdots & s_{N-1,J-1} \end{bmatrix} \tag{3.13}$$

where the n^{th} row represents the symbols transmitted in the n^{th} subcarrier and j^{th} column represents the symbols transmitted in the j^{th} time slot.

Each data symbol $s_{n,j}$ is up-sampled by zero-padding $JK-1$ zeros and is represented as

$$s_{n,j}(n) = s_{n,j}\delta(k - jK) \tag{3.14}$$

where K is the number of samples in a time-slot. This sequence is fed to a transmit filter with impulse response $p(k)$ of length $L = JK$ and circular convolution is performed. The last jK samples at the output of the filter are appended to the first jK position. The transmit filter can have non-rectangular shape which can be either raised cosine (RC) or root raised cosine (RRC) [18, 19].

After performing circular convolution, each sub-stream is up-converted by a complex subcarrier given by

$$c_n(k) = e^{\frac{-(i2\pi nk)}{K}} \tag{3.15}$$

The complex valued O-GFDM symbol can be written as

$$x(k) = \sum_{j=0}^{J-1}\sum_{n=0}^{N-1} s_{n,j}(k) \odot p(< k - jK >_{JK-1})c_n(k) \tag{3.16}$$

where $<>_Z$ denotes the Z-modulo operator and $\odot$ denotes the circular convolution. Equation (3.16) can be expressed as

$$x(k) = \sum_{j=0}^{J-1}\sum_{n=0}^{N-1} s_{n,j}p_j(k)c_n(k) \tag{3.17}$$

where

$$p_j(k) = p(< k - jK >_{JK-1}) \tag{3.18}$$

Equation (3.17) can be expressed in the following matrix form:

$$\mathbf{X} = diag(\mathbf{CSP}) \tag{3.19}$$

where diag (.) returns the main diagonal of a matrix,

$$\mathbf{C} = \begin{bmatrix} c_0(k)^T & c_1(k)^T & \dots & c_{n-2}(k)^T & c_{n-1}(k)^T \end{bmatrix} \tag{3.20}$$

is the matrix containing N complex subcarriers and

$$\mathbf{P} = \begin{bmatrix} p_0(k) \\ p_1(k) \\ p_2(k) \\ \vdots \\ p_{J-1}(k) \end{bmatrix} \tag{3.21}$$

is the matrix which contains the circular shifted version of p(k).

The complex valued OGFDM signal can also be represented as

$$\mathbf{X} = \mathbf{AD} \tag{3.22}$$

where

$$\mathbf{A} = \begin{bmatrix} p_0(k)c_0(k) \\ p_0(k)c_1(k) \\ \vdots \\ p_0(k)c_{N-1}(k) \\ p_1(k)c_0(k) \\ \vdots \\ p_{J-1}(k)c_{N-1}(k) \end{bmatrix}^T \tag{3.23}$$

is the transformation matrix and $\mathbf{D}$ is a serialized symbol vector which is given as

$$\mathbf{D} = \begin{bmatrix} s_{0,0} \\ s_{1,0} \\ \vdots \\ s_{N-1,0} \\ s_{0,1} \\ s_{1,1} \\ s_{2,1} \\ \vdots \\ s_{N-1,J-1} \end{bmatrix} \tag{3.24}$$

Cyclic prefix (CP) is added to the resultant complex O-GFDM signal. Further, this signal needs to be converted into real and positive for data transmission in optical wireless channel. To meet this requirement, the real and imaginary part of the complex valued signal $\mathbf{X}$ is separated and transmitted in different sub-frames. First sub-frame contains the real part of $\mathbf{X}$ and the second sub-frame which contains the imaginary part are frame multiplexed where real and imaginary part are represented as $\mathbf{X_1}$ and $\mathbf{X_2}$ i.e., $\mathbf{Re(X)}$,$\mathbf{Im(X)}$ respectively.

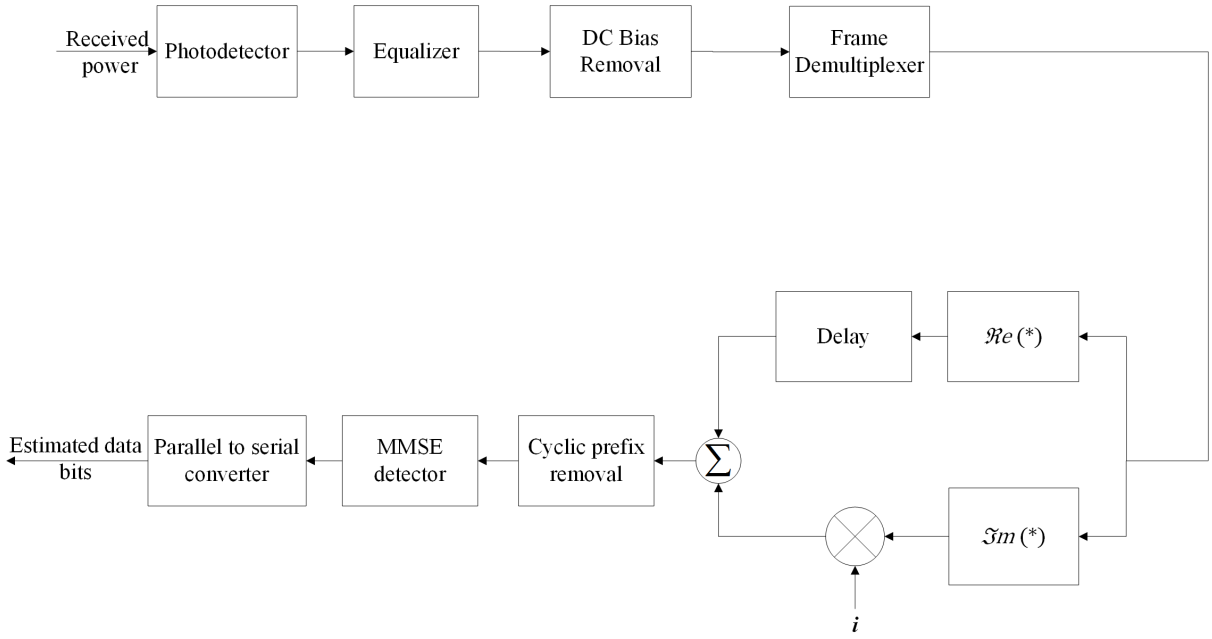

Figure 3.4: Block diagram of OGFDM-DC receiver.

After time multiplexing $\mathbf{X_1}$ and $\mathbf{X_2}$, we get the resultant vector $\mathbf{X_3}$ as follows

$$\mathbf{X_3} = \begin{bmatrix} \mathbf{X_1} \\ \mathbf{X_2} \end{bmatrix}^T \tag{3.25}$$

After adding a DC bias to the resultant signal,the unipolar signal is transmitted through the optical wireless channel.DC-biased O-GFDM bit rate is given by

$$R_{OGFDM-DC} = \frac{JN}{2(JT + T_{CP})} log_2 M \tag{3.26}$$

where T and T_{CP} are one time slot and CP duration respectively.

Receiver

The block diagram of the DC biased O-GFDM receiver is shown in Fig.3.4. Received optical signal is first converted into the electrical signal with the help of photo-detector.

After equalization and removal of DC bias, the resultant signal is further de-multiplexed to get back the complex valued signal $\mathbf{Y}$.

After removal of CP, minimum mean square error (MMSE) detector [20] is used to estimate the transmitted data bits $\mathbf{X_{MMSE}}$ which is given as

$$\mathbf{X_{MMSE}} = (\mathbf{A}^H \mathbf{A} + (\frac{1}{SNR})\mathbf{I}_{NJ})^{-1} \mathbf{A}^H \mathbf{Y} \tag{3.27}$$

where SNR is the signal to noise ratio of the channel and I_{NJ} is the identity matrix of size NJ.

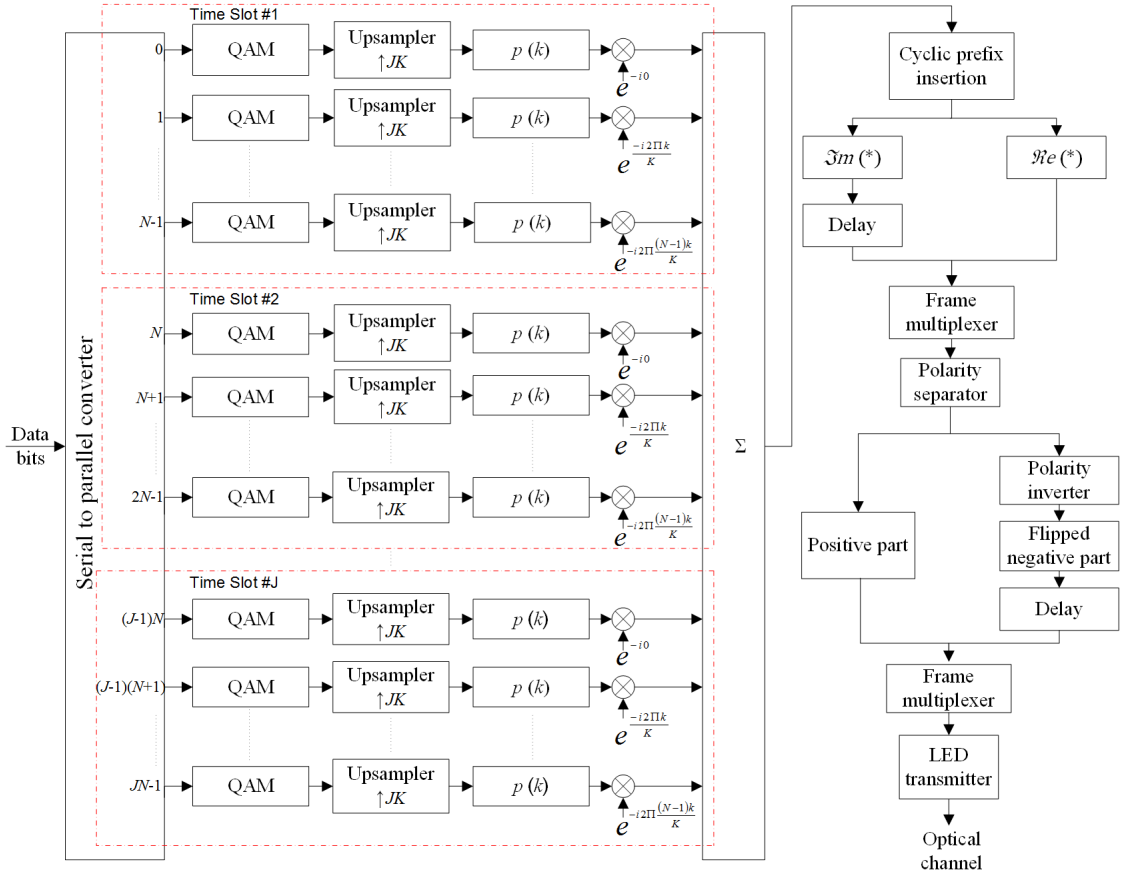

Figure 3.5: Block diagram of OGFDM-NDC transmitter.

3.3.2 OGFDM-NDC

In this paper, we propose an another transmission strategy borrowed from Flip-OFDM [21] and tailored for optical GFDM to support successive data transmission.The block diagram of the non-DC biased OGFDM transmitter is shown in fig.3.5

Transmitter

At the transmitter side, the processing till the formation of the bipolar signal is same as that of DC biased optical GFDM. Referring equation (13), the bipolar signal x_3 can be written as

$$x_3(k) = x_3^+(k) + x_3^-(k) \tag{3.28}$$

where $x_3^+(k)$ and $x_3^-(k)$ are the positive and negative parts of $x_3(k)$ respectively. It is defined as

$$x_3^+(k) = \begin{cases} x_3(k); x_3(k) \geq 0 \\ 0 \quad\quad ; otherwise \end{cases} \tag{3.29}$$

$$x_3^-(k) = \begin{cases} x_3(k); x_3(k) < 0 \\ 0 \quad\quad ; otherwise \end{cases} \tag{3.30}$$

Positive part $\mathbf{X_3^+}(k)$ is transmitted in first OGFDM sub-frame while the second sub-frame carries the flipped (inverted polarity) signal $(-\mathbf{X_3^-}(k))$ and then they are frame multiplexed. All the samples of the resultant signal are now unipolar and the signal is transmitted through the optical

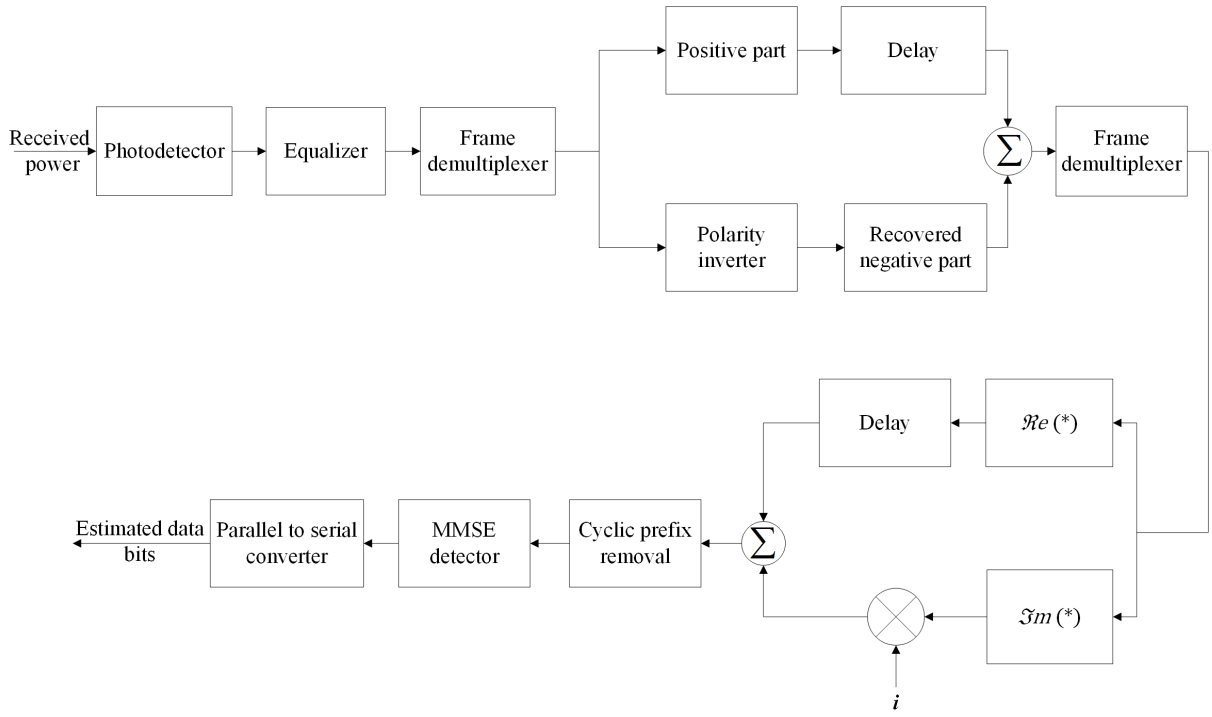

Figure 3.6: Block diagram of OGFDM-NDC receiver.

wireless channel using LED.Non-DC biased OGFDM bit rate is given by

$$R_{OGFDM-NDC} = \frac{JN}{4(JT + T_{CP})} log_2 M \tag{3.31}$$

where T and T_{CP} are one time slot and CP duration respectively.

Receiver

The block diagram of the non-DC biased O-GFDM receiver is shown in Fig.3.6. Received optical signal is first converted into the electrical signal with the help of photo-detector.

After equalization, bipolar signal Y_1 is regenerated as

$$\mathbf{Y_1} = \mathbf{Y_1^+} - \mathbf{Y_1^-} \tag{3.32}$$

where Y_1^+ is the first sub-frame and Y_1^- is the second sub-frame received after frame demulti-

plexing. Resultant Y_1 is further de-multiplexed to get back the complex valued signal Y.

After removal of CP, minimum mean square error (MMSE) detector [20] is used to estimate the transmitted data bits X_{MMSE}(referring equation 3.27).

Chapter 4

DFT Precoded Optical OFDM

4.1 DFT precoded optical OFDM

Since DCO-OFDM is less power efficient. It has high peak to average power ratio. There is a need for a modulation technique which should be more power efficient with good SER performance. Block diagram of DFT precoded optical OFDM technique is shown in Fig.4.1. In this technique, data bits are quadrature amplitude modulated. N number of subcarriers are used which carry the data in the frequency domain. A low pass FIR Gaussian pulse shaping filter is used. Filter coefficients have been calculated with consideration of even numbered order and 3-dB bandwidth- symbol time product (BT)= 0.5. Each coefficient gets multiplied with its respective data point. In a summarized way, it can be said that a Gaussian pulse act as carrier whose amplitude is modified according to the data carried by subcarriers in frequency domain. The real and imaginary part of the resultant modified signal is separated out in time domain and stored into the different frames and frame multiplexing is done.This is done to make the transmitted signal real. DC bias is added to make the real valued signal positive since real and positive valued signal is needed in intensity modulation and direct detection. This technique has low peak to average power ratio as well as very good SER performance.

At the receiver side, received optical power is converted into the electrical signal with the help of photodetector. After channel equalization, DC bias is removed. After frame demultiplexing, complex valued signal is reconstructed. Frequency domain equalizer is used to get back the information. [22]

The parameters like spectral efficiency, complexity etc. are yet to be investigated for this scheme.

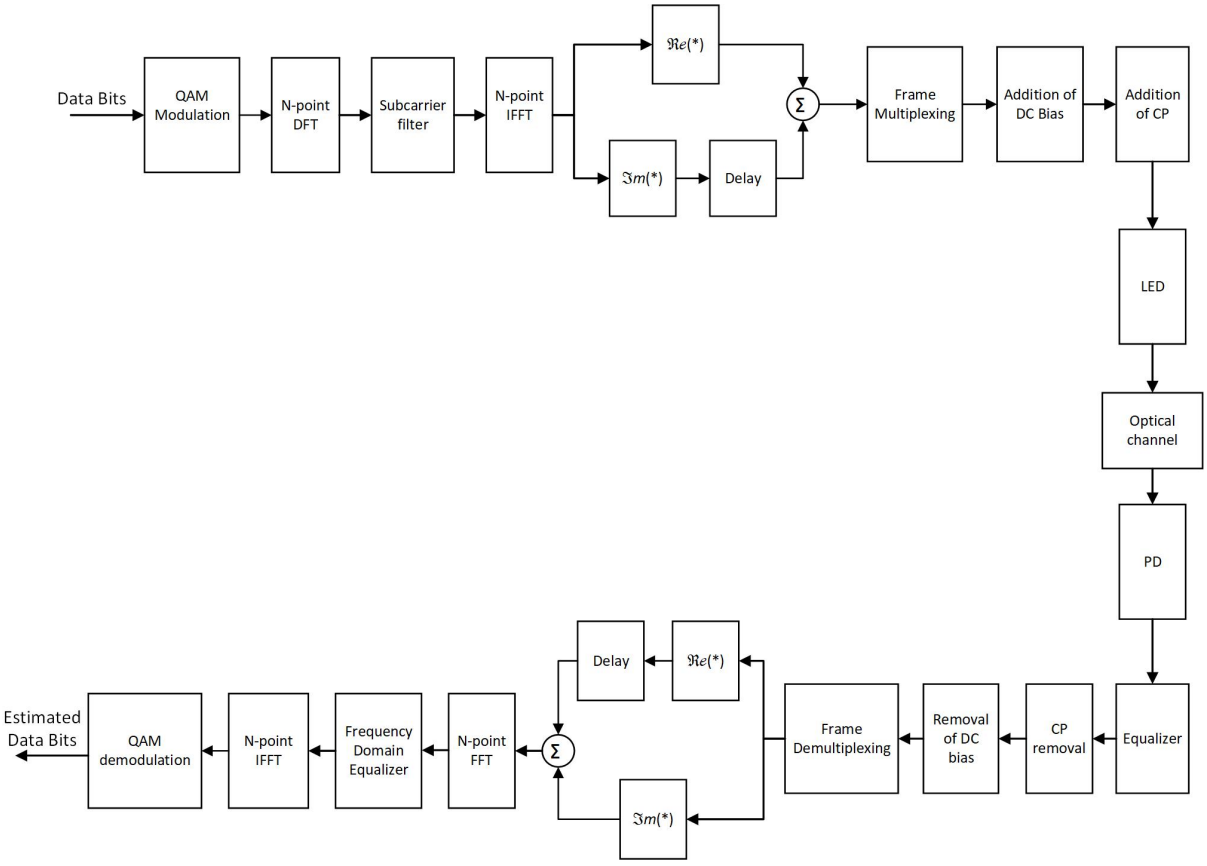

Figure 4.1: Block diagram of DFT precoded optical OFDM.

Chapter 5

Mathematical analysis of Spectral efficiency

This chapter includes the mathematical analysis of spectral efficiency of DCO-OFDM, ACO-OFDM and OGFDM modulation schemes.

Hermitian symmetry is used in DCO-OFDM, therefore information is carried by only half subcarriers. Therefore, the bit rate of DCO-OFDM is given by

$$R_{DCO} = \frac{N/2}{(T + T_{CP})} log_2 M \tag{5.1}$$

where T and T_{CP} are one time slot and CP duration respectively and M is the modulation level. However,ACO-OFDM utilizes only odd number of subcarriers to carry data. Information is present only half of the odd number of subcarriers. Hence, ACO-OFDM bit rate is given by

$$R_{ACO} = \frac{N/4}{(T + T_{CP})} log_2 M \tag{5.2}$$

The spectral efficiency gain of ACO-OFDM over DCO-OFDM can be calculated as

$$\eta_1 = \frac{R_{ACO}}{R_{DCO}} = \frac{1}{2} \tag{5.3}$$

In this way, spectral efficiency of ACO-OFDM gets halved compared to DCO-OFDM. OGFDM-DC and OGFDM-NDC modulation schemes add CP after every J time slots, unlike ACO-OFDM and DCO-OFDM which require CP addition after one time slot. Thus, OGFDM-DC bit rate is given by

$$R_{OGFDM-DC} = \frac{JN}{2(JT + T_{CP})} log_2 M \tag{5.4}$$

Similarly, bit rate of OGFDM-NDC is given by

$$R_{OGFDM-NDC} = \frac{JN}{4(JT + T_{CP})} log_2 M \tag{5.5}$$

Spectral efficiency gain of OGFDM-DC over DCO-OFDM can be calculated as

$$\eta_2 = \frac{R_{OGFDM-DC}}{R_{DCO}} = \left(\frac{1 + \frac{T_{CP}}{T}}{1 + \frac{T_{CP}}{JT}} \right) \tag{5.6}$$

Similarly, the spectral efficiency gain of OGFDM-NDC over DCO-OFDM is given by

$$\eta_3 = \frac{R_{OGFDM-NDC}}{R_{DCO}} = \frac{(1 + \frac{T_{CP}}{T})}{2(1 + \frac{T_{CP}}{JT})} \tag{5.7}$$

For same number of subcarriers,same modulation order and $\frac{T_{CP}}{T} = 0.1$, spectral efficiency gain of OGFDM-DC amd OGFDM-NDC is found to be 1.07 and 0.53 respectively. Thus it can be concluded that OGFDM-DC has best spectral efficiency among four schemes.

Chapter 6

Simulation and Results

This chapter comprises the comparison of OGFDM-DC with DCO-OFDM and OGFMD-NDC with ACO-OFDM, based on their SER, PAPR performance. Various simulation parameters are shown in Table 6.1 . Simulations are done by considering the parameters such that OGFDM, ACO-OFDM and DCO-OFDM have the same spectral efficiency. For this case, total number of timeslots J for OGFDM is 1.

6.0.1 SER

SER performance of OGFDM-DC and DCO-OFDM for optical LOS channel is shown in Fig.6.1. It is observed that SER performance of OGFDM-DC is better than the DCO-OFDM.OGFDM-DC provides a SNR gain of around 8 dB over DCO-OFDM for FEC limit (SER of 10^{-3}). Fig.6.2 shows the SER performance of OGFDM-NDC and ACO-OFDM. The performance of OGFDM-NDC closely approaches to ACO-OFDM. However, the minor difference in SER performance of OGFDM-NDC is due to the non-orthogonality of subcarriers. This difference is insignificant over the benefit of spectral efficiency while using OGFDM-NDC.

Table 6.1: Simulation Parameter Sets for O-GFDM and O-OFDM

Parameters	**ACO-OFDM/DCO-OFDM**	**OGFDM-DC/OGFDM-NDC**
Number of subcarriers	128/64	4/8
Constellation Order	4	4
Upsampling factor	NA	4
Signal bandwidth	20 MHz	20 MHz
Transmit Filter	NA	RRC
Roll off factor	NA	0.1

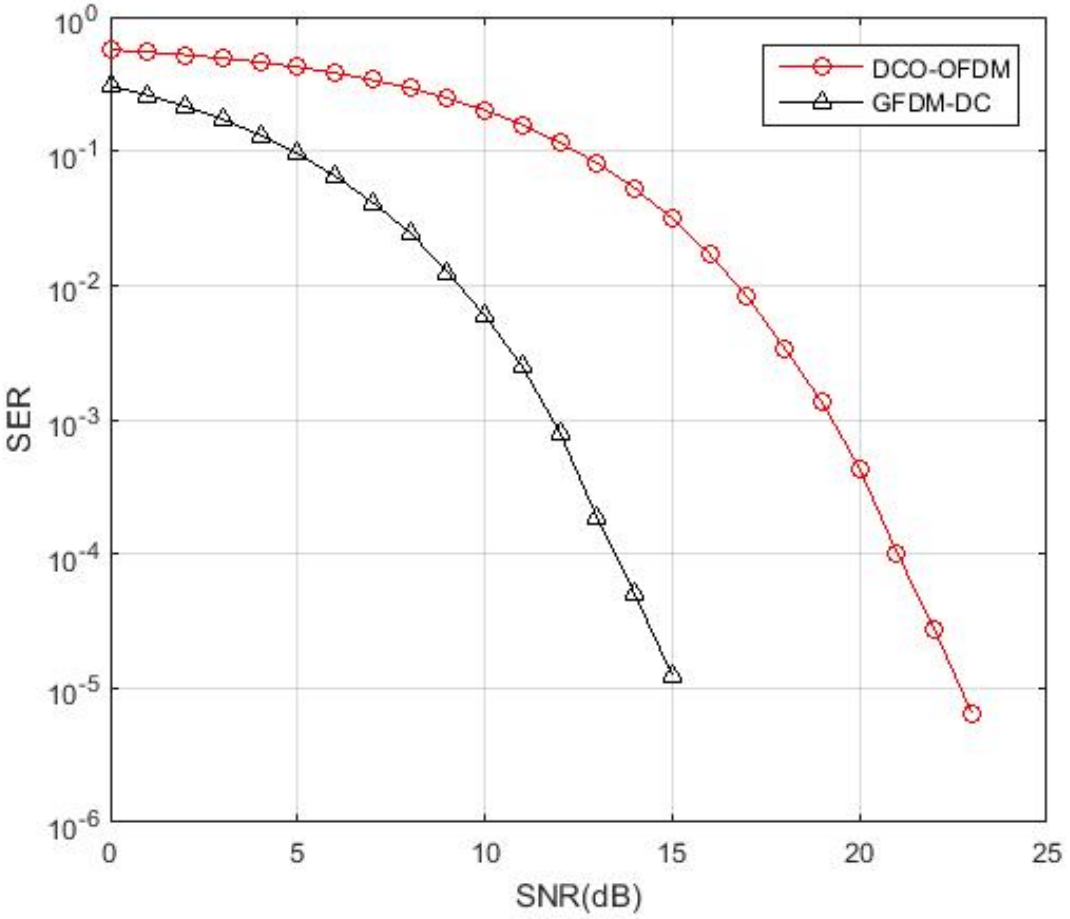

Figure 6.1: SER performance of OGFDM-DC and DCO-OFDM.

6.0.2 PAPR

Peak-to-average-power-ratio (PAPR) of a transmitted signal x(t) can be defined as

$$PAPR = \frac{max[x(t)x^*(t)]}{E[x(t)x^*(t)]} \tag{6.1}$$

A high PAPR signal requires LEDs with large dynamic range for avoiding the clipping distortion. The probability of PAPR to be greater than the threshold value ($PAPR_o$) is defined by complementary cumulative distribution function (CCDF). CCDF curves for OGFDM-DC and DCO-OFDM is shown in Fig.6.3. OGFDM-DC exhibits a superior performance compared to DCO-OFDM. Fig.6.4 shows CCDF curves for OGFDM-NDC and ACO-OFDM, it is observed that the OGFDM-NDC has a better PAPR reduction compared to ACO-OFDM. This reduced PAPR of OGFDM-DC and OGFDM-NDC, makes them power efficient.

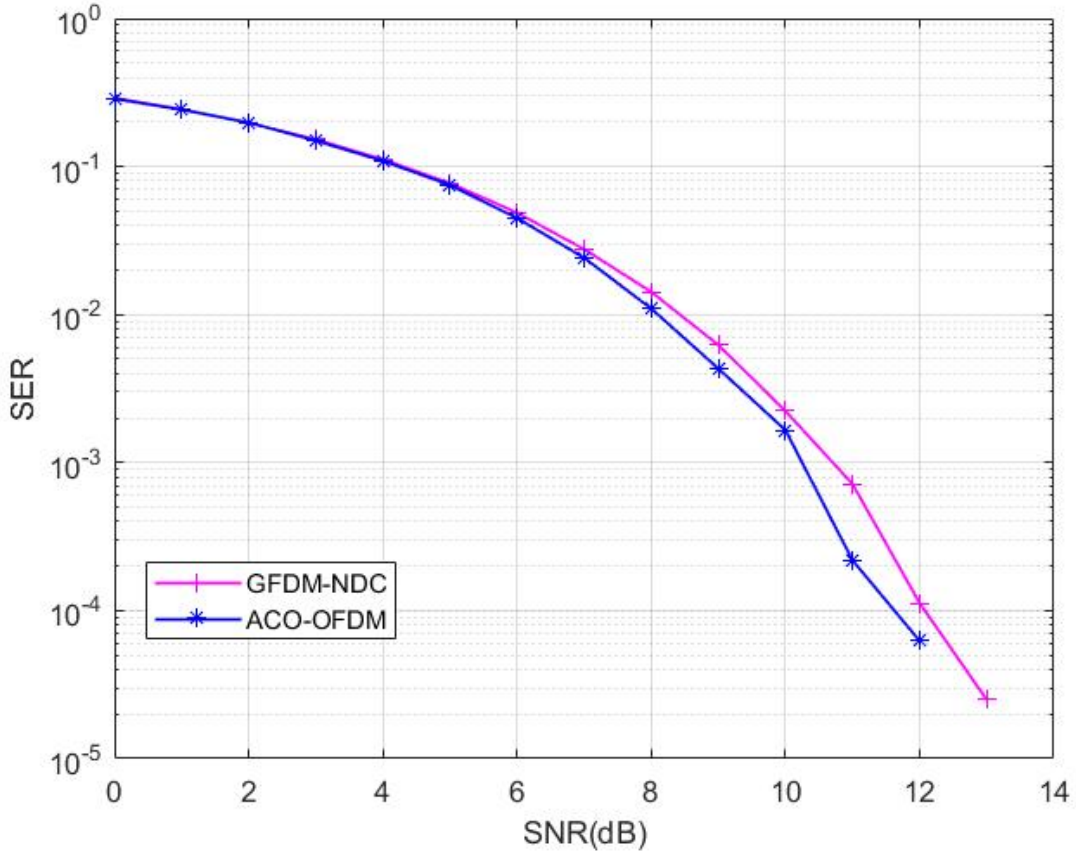

Figure 6.2: SER performance of OGFDM-NDC and ACO-OFDM.

6.0.3 Complexity

If we compare the O-OFDM schemes with O-GFDM schemes in terms of complexity then it can be observed from the Figs.6.5 and 6.6 that more number of complex multiplications are required in OGFDM as compared to O-OFDM at the transmitter and receiver side.

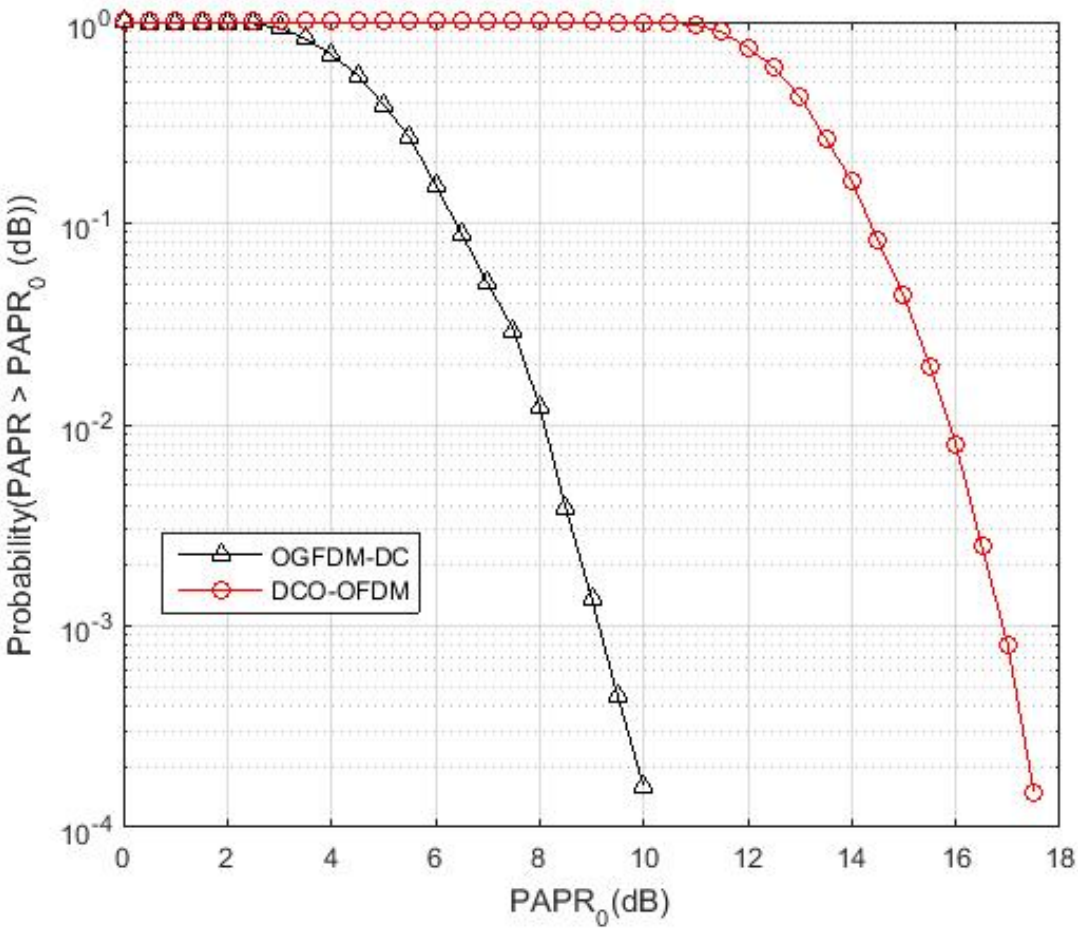

Figure 6.3: CCDF distribution of PAPR for OGFDM-DC and DCO-OFDM.

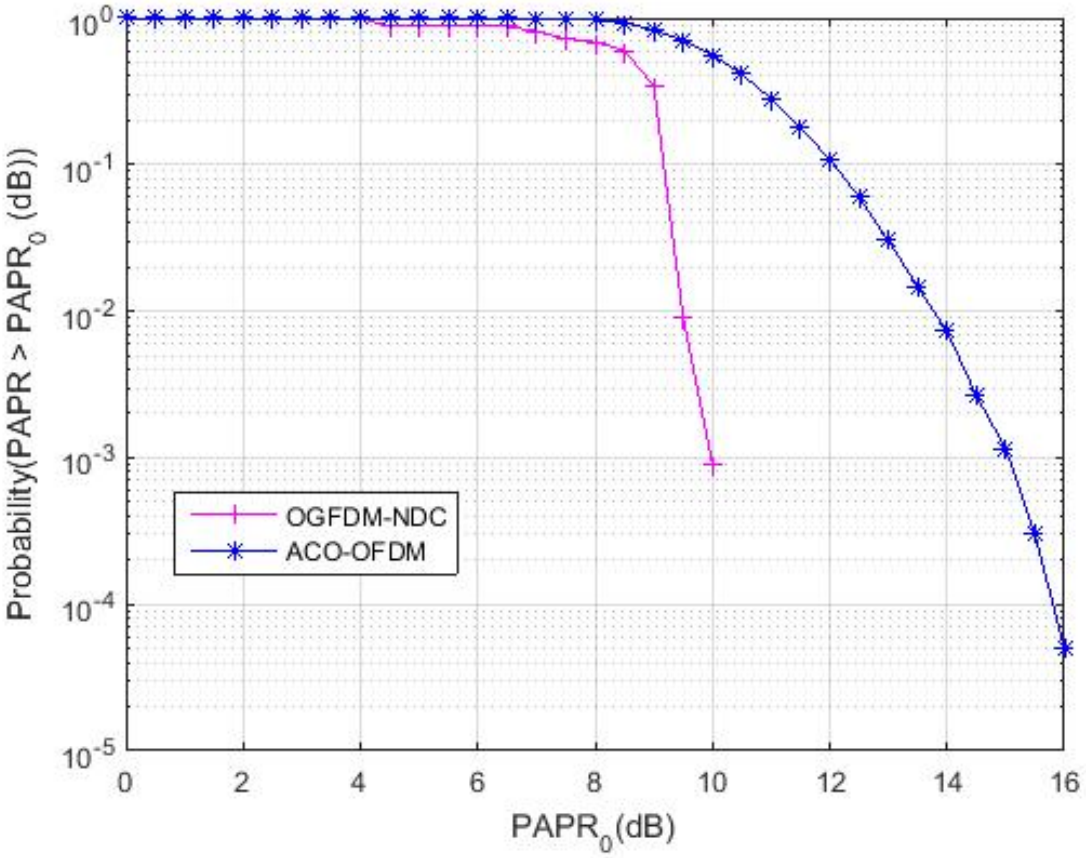

Figure 6.4: CCDF distribution of PAPR for OGFDM-NDC and ACO-OFDM.

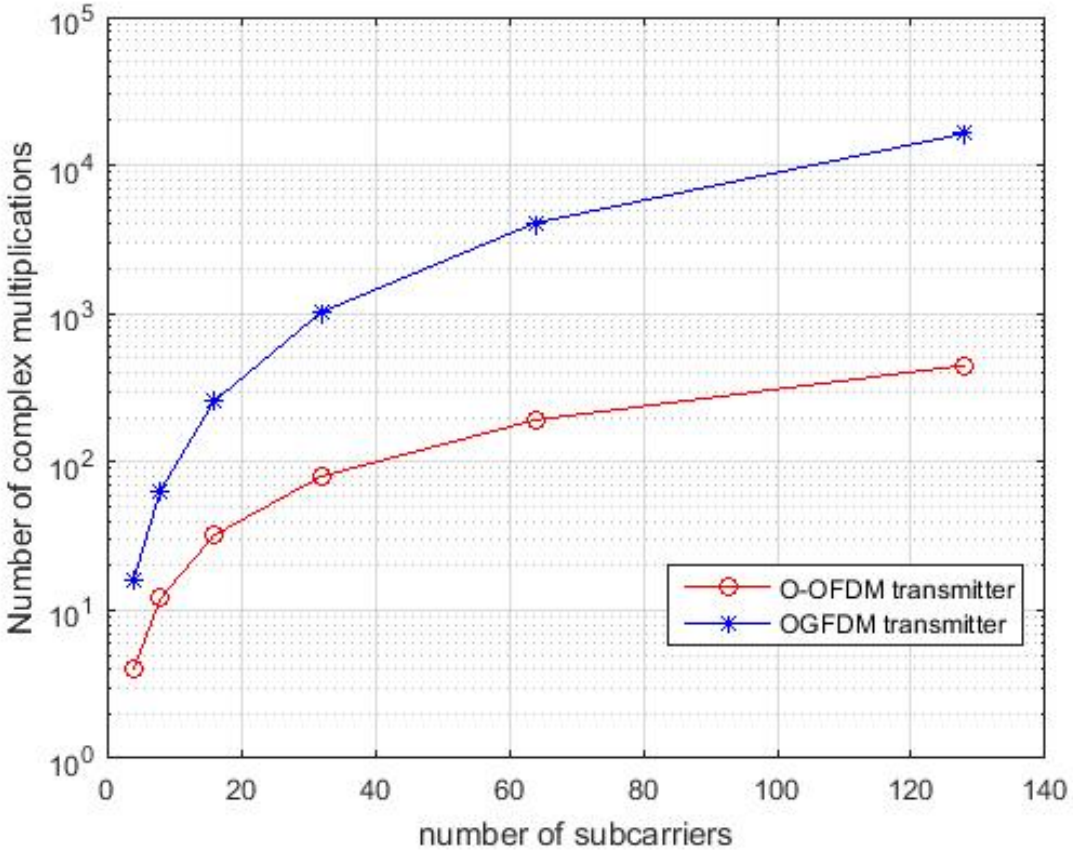

Figure 6.5: Number of subcarriers vs number of complex multiplication at the transmitter side

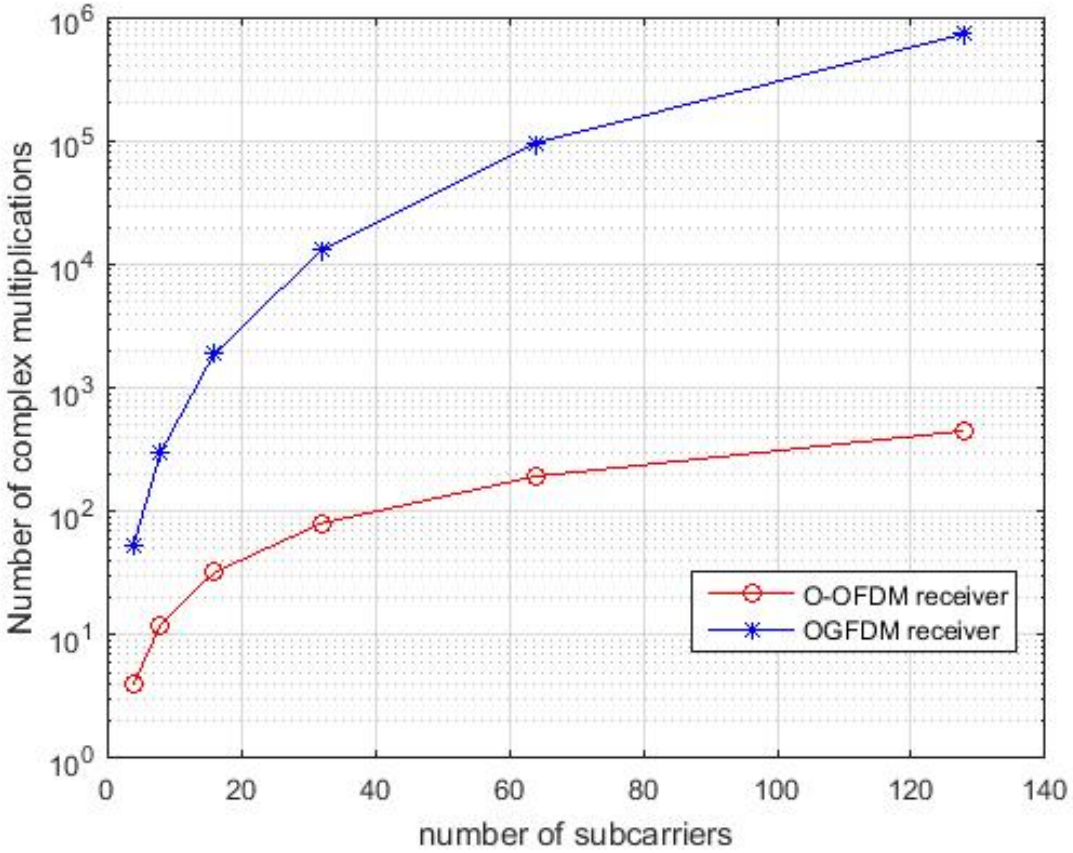

Figure 6.6: Number of subcarriers vs number of complex multiplication at the receiver side

Table 6.2: Simulation Parameter Sets for proposed scheme and DCO-OFDM

Parameters	**DCO-OFDM**	**Proposed scheme**
Number of subcarriers	64	64
Constellation Order	4	4
Signal bandwidth	20 MHz	20 MHz
BT factor(Gaussian pulse shape)	NA	0.5

6.1 Simulation results of proposed modulation scheme

This chapter also comprises the simulation results of proposed modulation scheme. Comparison is done between this scheme and DCO-OFDM in terms of SER and PAPR performance.The simulation parameters are given in the Table 6.2.

6.1.1 SER

SER performance of proposed scheme and DCO-OFDM for optical LOS channel is shown in Fig.6.7. It is observed that SER performance of proposed scheme is better than the DCO-OFDM. Proposed scheme provides a SNR gain of around 6 dB over DCO-OFDM for FEC limit (SER of 10^{-3}).

6.1.2 PAPR

To avoid the clipping distortion, a high PAPR signal requires LEDs with large dynamic range. The probability of PAPR to be greater than the threshold value ($PAPR_o$) is defined by complementary cumulative distribution function (CCDF). CCDF curves for proposed scheme and DCO-OFDM is shown in Fig.6.8. The proposed scheme exhibits a superior performance compared to DCO-OFDM.Reduced PAPR of proposed scheme makes it power efficient.

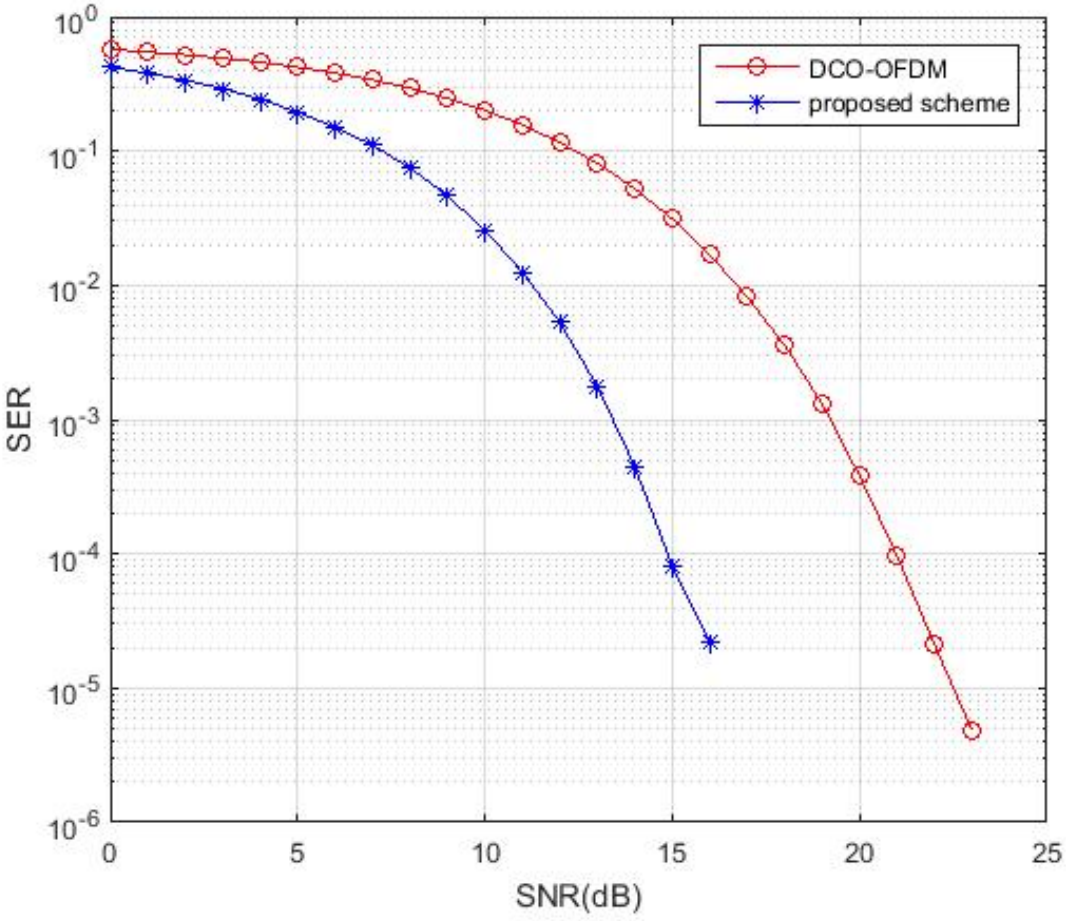

Figure 6.7: SER performances of proposed scheme and DCO-OFDM

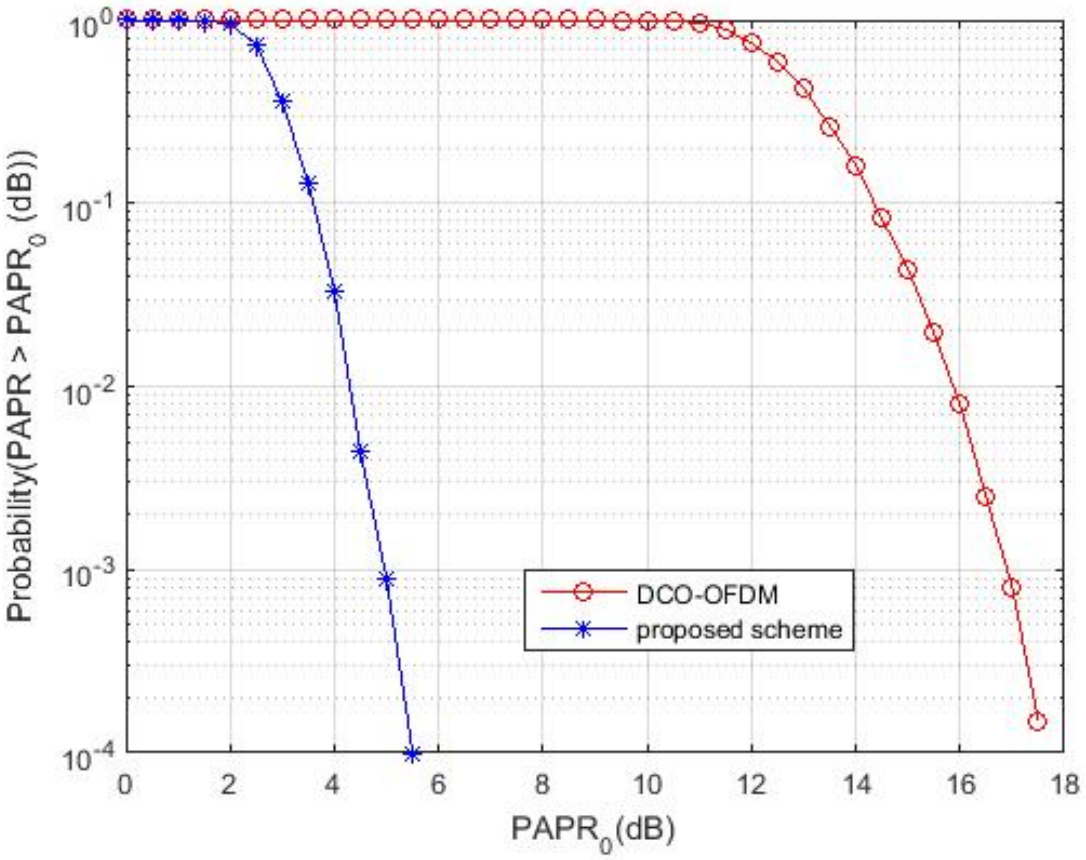

Figure 6.8: CCDF distribution of PAPR for proposed scheme and DCO-OFDM

Conclusion

This thesis work proposed OGFDM schemes for VLC and these are evaluated on the basis of their symbol error rate performance, PAPR and spectral efficency.The comparison has been done with existing DCO-OFDM and ACO-OFDM schemes in context of certain parameters such as symbol error rate performance, PAPR and spectral efficiency.we conclude that proposed OGFDM-DC has better SER performance compared to DCO-OFDM.OGFDM-NDC has SER performance matching to ACO-OFDM. There is a huge reduction in PAPR for both OGFDM-DC and OGFDMNDC compared with existing DCO-OFDM and ACO-OFDM, which makes OGFDM robust against the clipping distortion introduced due to LED non-linearity. Also the proposed scheme has better spectral efficiency. OGFDM can become an improved alternative to ACO-OFDM and DCO-OFDM. As GFDM is being actively considered by wireless community for LTE-A like 5G systems and has the advantage of simple transmit and receive waveform, less hardware cost and power consumption due to its low PAPR. This type of next generation cellular communication will very well gel with OGFDM based VLC to deliver seamless end-to-end communication system and will provide greater flexibility to optimize the network using software defined networking.

DFT precoded optical OFDM is implemented for indoor VLC which is compared with DCO-OFDM and this scheme has the better SER performance along with huge reduction in PAPR in comparison to DCO-OFDM. Some parameters like complexity, spectral efficiency etc. are yet to be investigated for this scheme.

Bibliography

[1] D. Karunatilaka, F. Zafar, V. Kalavally, and R. Parthiban, "Led based indoor visible light communications: State of the art.," *IEEE Communications Surveys and Tutorials*, vol. 17, no. 3, pp. 1649–1678, 2015.

[2] A. G. Bell, W. Adams, W. Preece, *et al.*, "Discussion on" the photophone and the conversion of radiant energy into sound"," *Journal of the Society of Telegraph Engineers*, vol. 9, no. 34, pp. 375–383, 1880.

[3] D. K. Jackson, T. K. Buffaloe, and S. B. Leeb, "Fiat lux: A fluorescent lamp digital transceiver," *IEEE Transactions on industry applications*, vol. 34, no. 3, pp. 625–630, 1998.

[4] C. Medina, M. Zambrano, and K. Navarro, "Led based visible light communication: Technology, applications and challenges-a survey," *International Journal of Advances in Engineering & Technology*, vol. 8, no. 4, p. 482, 2015.

[5] Y. Tanaka, S. Haruyama, and M. Nakagawa, "Wireless optical transmissions with white colored led for wireless home links," in *Personal, Indoor and Mobile Radio Communications, 2000. PIMRC 2000. The 11th IEEE International Symposium on*, vol. 2, pp. 1325–1329, IEEE, 2000.

[6] S. Zhao, J. Xu, and O. Trescases, "A dimmable led driver for visible light communication (vlc) based on llc resonant dc-dc converter operating in burst mode," in *Applied Power Electronics Conference and Exposition (APEC), 2013 Twenty-Eighth Annual IEEE*, pp. 2144–2150, IEEE, 2013.

[7] "Led spectra." `https://commons.wikimedia.org/wiki/File:Red-YellowGreen-Blue_LED_spectra.png`.

[8] "White led spectra." `https://en.wikipedia.org/wiki/Light-emitting_diode#/media/File:White_LED.png`.

[9] K. Minolta, "Oled lighting." `http://www.konicaminolta.com/oled/products/index.html`.

[10] S. Fotios, "Lighting in offices: lamp spectrum and brightness," *Coloration Technology*, vol. 127, no. 2, pp. 114–120, 2011.

[11] M. Z. Afgani, H. Haas, H. Elgala, and D. Knipp, "Visible light communication using ofdm," in *Testbeds and Research Infrastructures for the Development of Networks and Communities, 2006. TRIDENTCOM 2006. 2nd International Conference on*, pp. 6–pp, IEEE, 2006.

[12] M. Zhang and Z. Zhang, "An optimum dc-biasing for dco-ofdm system," *IEEE Communications Letters*, vol. 18, no. 8, pp. 1351–1354, 2014.

[13] J. Armstrong and B. J. Schmidt, "Comparison of asymmetrically clipped optical ofdm and dc-biased optical ofdm in awgn," *IEEE Communications Letters*, vol. 12, no. 5, 2008.

[14] J. Armstrong and A. Lowery, "Power efficient optical ofdm," *Electronics Letters*, vol. 42, no. 6, pp. 370–372, 2006.

[15] J. Armstrong, B. J. Schmidt, D. Kalra, H. A. Suraweera, and A. J. Lowery, "Spc07-4: Performance of asymmetrically clipped optical ofdm in awgn for an intensity modulated direct detection system," in *Global Telecommunications Conference, 2006. GLOBECOM'06. IEEE*, pp. 1–5, IEEE, 2006.

[16] X. Li, R. Mardling, and J. Armstrong, "Channel capacity of im/dd optical communication systems and of aco-ofdm," in *Communications, 2007. ICC'07. IEEE International Conference on*, pp. 2128–2133, IEEE, 2007.

[17] N. Fernando, Y. Hong, and E. Viterbo, "Flip-ofdm for unipolar communication systems," *IEEE Transactions on Communications*, vol. 60, no. 12, pp. 3726–3733, 2012.

[18] B. M. Alves, L. L. Mendes, D. A. Guimaraes, and I. S. Gaspar, "Performance of gfdm over frequency-selective channels-invited paper," in *Proc. International Workshop on Telecommunications, 2013.*, 2013.

[19] G. Fettweis, M. Krondorf, and S. Bittner, "Gfdm-generalized frequency division multiplexing," in *Vehicular Technology Conference, 2009. VTC Spring 2009. IEEE 69th*, pp. 1–4, IEEE, 2009.

[20] N. Michailow, S. Krone, M. Lentmaier, and G. Fettweis, "Bit error rate performance of generalized frequency division multiplexing," in *Vehicular Technology Conference (VTC Fall), 2012 IEEE*, pp. 1–5, IEEE, 2012.

[21] N. Fernando, Y. Hong, and E. Viterbo, "Flip-ofdm for optical wireless communications," in *Information Theory Workshop (ITW), 2011 IEEE*, pp. 5–9, IEEE, 2011.

[22] K. Kuchi, "Partial response dft-precoded-ofdm modulation," *Transactions on Emerging Telecommunications Technologies*, vol. 23, no. 7, pp. 632–645, 2012.